Robotica (2023), **41**, pp. 587–608
doi:10.1017/S0263574722001448

CAMBRIDGE UNIVERSITY PRESS

RESEARCH ARTICLE

Grasp compliance achieved with a planar hand composed of multiple 3-joint fingers

Shuguang Huang* and Joseph M. Schimmels

Department of Mechanical Engineering, Marquette University, Milwaukee, WI, USA
*Corresponding author. E-mail: huangs@marquette.edu

Received: 5 May 2022; **Revised:** 22 July 2022; **Accepted:** 13 September 2022; **First published online:** 10 October 2022

Keywords: compliance realization, robotic hands, grasp compliance

Abstract

In this paper, the realization of any specified planar Cartesian compliance for an object grasped by a compliant hand is addressed. The hands considered have 2 or more fingers for which each has 3 modulated elastic joints and predetermined link lengths. Geometric construction-based compliance synthesis procedures are developed. Using these procedures, a large set of compliant behaviors can be realized by a single hand simply by adjusting the configuration of each finger and by adjusting the joint stiffness (using variable stiffness actuation) of each finger joint.

1. Introduction

Compliance is widely used in robotic manipulation to improve the accuracy of constrained relative positioning and to prevent excessive contact forces when interacting with its environment. Robot dexterity is greatly enhanced when its compliance is properly structured for each constrained manipulation task [1, 2]. Different tasks require different compliant behaviors. Dexterous manipulation can be attained for many different tasks with a single robot if the robot is capable of changing its task-specific compliance in real time.

A general model for compliance is a rigid body suspended by a set of elastic components. A compliant behavior is characterized by the relationship between the force and torque exerted on the body and the resulting deflection of the body. For small deflections, if the body motion is represented by a screw displacement, twist $\mathbf{t}$, and the force and torque are represented by a screw wrench $\mathbf{w}$, then the relationship is linear and can be described as:

$$\mathbf{w} = \mathbf{K}\mathbf{t}, \tag{1}$$

where $\mathbf{K}$ is the symmetric positive semi-definite (PSD) *stiffness* matrix. For a full-rank suspension, $\mathbf{K}$ is positive definite (PD), and Eq. (1) can be equivalently expressed as:

$$\mathbf{t} = \mathbf{C}\mathbf{w}, \tag{2}$$

where $\mathbf{C} = \mathbf{K}^{-1}$ is the *compliance* matrix.

In application, an elastic suspension of a body can be attained by a compliant mechanism composed of elastic components connected in parallel or in series. To realize a desired compliance, both the geometry and elastic behavior of each component need to be appropriately selected. This paper focuses on compliance realization with a planar compliant hand, which is composed of multiple elastic serial mechanisms (fingers having elastic joints) connected in parallel to a base (the palm) as shown in Fig. 1. Each finger considered has 3 joints with modulated stiffness (using variable stiffness actuation [3]) and each fingertip contacts the surface of the body so that a desired elastic behavior is attained by the body.

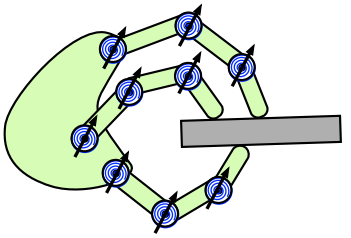

Figure 1. *Compliant robotic hand with multiple 3-joint fingers. Each finger has 3 individually modulated elastic joints. The object is held by the fingers in point contact.*

Due to the kinematic redundancy of each finger, a hand has the ability to grasp objects of many different shapes and to grasp/regrasp an object to achieve different elastic behaviors. For a given hand, a continuous space of compliances can be achieved by adjusting the finger joint compliances and varying the fingertip locations on the object surface without changing the pose of the held object.

1.1. Related work

In previous work on the realization of compliance, synthesis procedures for compliant mechanisms have been developed to achieve any specified elastic behavior. Most early synthesis procedures were developed for fully parallel mechanisms and fully serial mechanisms based on a rank-1 decomposition of the stiffness/compliance matrix [4, 5, 6, 7].

In refs. [8, 9], methods of stiffness synthesis using planar parallel mechanisms with specific constructions were developed. In refs. [10, 11, 12, 13], compliance analysis and synthesis for mechanisms composed of distributed elastic elements were presented.

In closely related prior work in the synthesis of *planar* compliance [14, 15, 16, 17], construction-based approaches to the design of fully serial or fully parallel mechanisms having n ($3 \leq n \leq 6$) elastic components were developed. In refs. [14, 18], the concepts of *dual elastic mechanisms* in serial and parallel construction were introduced for the realization of planar [14] and spatial [18] compliance. It was shown that the space of realizable compliances obtained by only adjusting joint compliances at a given serial mechanism configuration is exactly the same as that of its parallel elastic dual obtained by only adjusting spring stiffnesses. Thus, a serial mechanism can be replaced by its parallel elastic dual (and vice versa) in synthesis procedures for the realization of a specified elastic behavior. In ref. [19], the concept of dual elastic mechanisms was extended to non-full-rank cases.

In more recent work [20], the synthesis of an arbitrary planar compliance has been developed for mechanisms composed of multiple 3R serial compliant arms *rigidly connected* in parallel to a single body.

Many researchers addressed the analysis and synthesis of Cartesian compliance associated with an object held by a robotic hand [21, 22, 23, 24, 25, 26, 27, 28]. Most work has concentrated on the calculation of the Cartesian compliance of a given grasp. To approximate a specified object Cartesian compliance, numerical search procedures [21, 27] or optimization procedures [23, 26] have been used. In our most recent work [29], exact compliance realization was addressed for a planar hand having multiple 2-joint fingers in which finger link lengths were *unspecified*. In most prior work, fingers were modeled as rigid links connected in series by compliant joints. In refs. [30, 31], finite element methods were used to model and analyze a hand grasp.

1.2. Contribution of the paper

This paper addresses the exact realization of an arbitrary planar compliance with a multi-finger hand in which each finger has 3 elastic joints and *predetermined* rigid link lengths.

https://doi.org/10.1017/S0263574722001448 Published online by Cambridge University Press

In the synthesis of a desired elastic behavior for an object held by a compliant hand, the main limitations of prior work are (1) the numerical approaches presented in refs. [21, 27, 23, 26] did not take into account the geometric restrictions on each finger and did not guarantee that the desired compliance is actually achieved and (2) the synthesis procedure developed in ref. [29] did not consider the restriction of specified link lengths in each finger. Thus, due to kinematic limitations, the compliant hand determined by the procedure for a given compliance is very unlikely to be used for the realization of a different compliance.

This paper addresses the realization of an arbitrary planar compliance with a robotic hand having multiple 3-joint fingers in which finger base locations and link lengths are specified. The main contributions of the paper are

1. The development of a means to exactly realize a desired planar compliance for a held object with a *given* hand;
2. The development of geometry-based synthesis procedures for m ($m \geq 2$) finger planar hands that guarantee the realization of *any realizable* compliant behavior by the hand.

As previously stated, although constrained by hand geometry, a large, continuous space of compliant behaviors can be achieved by adjusting the joint compliance of each finger joint and changing the location where each fingertip contacts the held object.

1.3. Overview

This paper develops an approach to realizing an arbitrary planar (3×3) compliance matrix for an object held by a given compliant hand having 2 or more fingers for which each has 3 modulated passive compliant joints.

The paper is outlined as follows. In Section 2, the technical background needed for the realization of an elastic behavior with a mechanism is reviewed. In Section 3, the description of the compliance provided to a held object when in point contact with an elastic finger is addressed. Analysis and realization of general point stiffness associated with a fully parallel mechanism and of general point compliance associated with a fully serial mechanism are presented. In Section 4, compliance realization with a two or more finger hand in which the link lengths of each finger are predetermined is addressed. As such, the procedures can be applied to any given hand to synthesize an arbitrary compliant behavior. In Section 5, a numerical example is provided to demonstrate the synthesis procedures. Finally, a brief summary is presented in Section 6.

2. Technical background

In this section, the background needed for planar compliance realization with a compliant hand is provided. First, the specific model of a compliant grasp used in the paper is described. Next, screw representation of mechanism elastic characterization is reviewed. Finally, the limitation on the traditional approach to calculate grasp stiffness is described.

2.1. Model of a compliant grasp

In a hand, each finger/object combination can be viewed as a serial mechanism. A compliant grasp then can be modeled as a system of serial mechanisms connected in parallel to the held object. Unlike the fully serial mechanisms studied in previous work [15, 16, 17], in which the connection between links are all elastic revolute joints, the fingertip makes a hard point contact connection to the held body. As such, at the point of contact, only force (no torque) can be transmitted to the body as illustrated in Fig. 2(a).

It can be seen that, with the above assumptions, each finger can provide only point compliance to the body (yielding a rank deficient planar stiffness matrix at the contact point) regardless of number of the compliant joints in the finger. Since the fingertip does not transmit torque, the connection between the

https://doi.org/10.1017/S0263574722001448 Published online by Cambridge University Press

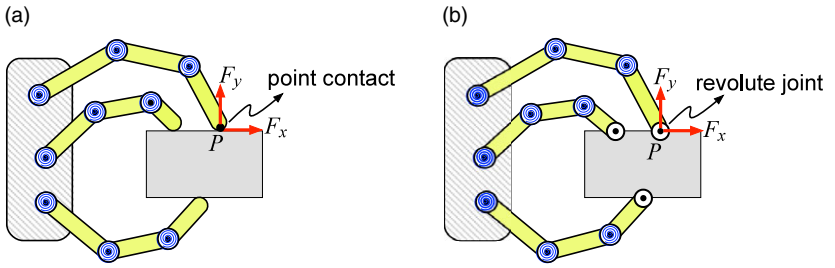

Figure 2. *Model of a compliant robotic hand with multiple 3-joint fingers. The fingertip of each finger only provides pure force (no torque) at the contact point and is modeled as a revolute joint without elastic behavior.*

finger tip and the object it contacts is equivalent to a free revolute joint at the contact point as shown in Fig. 2(b). Thus, when in contact with the held object, each 3-joint finger can be viewed as a 4*R* serial mechanism with the last joint having no elastic behavior.

2.2. Screw representation of mechanism geometry

Consider a fully parallel mechanism consisting of n line springs. The position of each spring can be represented by a unit wrench defined as the *spring wrench*. In Plücker ray coordinates, a planar line spring wrench has the form:

$$\mathbf{w} = \begin{bmatrix} \mathbf{n} \\ d \end{bmatrix}, \tag{3}$$

where the unit 2-vector $\mathbf{n}$ indicates the direction of the wrench (spring axis) and where

$$d = (\mathbf{r} \times \mathbf{n}) \cdot \mathbf{k}, \tag{4}$$

where $\mathbf{r}$ is the position vector from the origin to any point on the spring axis, and $\mathbf{k}$ is the unit vector orthogonal to the plane. Conversely, a unit wrench $\mathbf{w}$ in the form of Eq. (3) can be used to represent a line in the plane.

If a stiffness matrix $\mathbf{K}$ is passively realized with a parallel mechanism having n springs $\mathbf{w}_i$ $(1, \ldots, n)$, then [32]

$$\mathbf{K} = k_1 \mathbf{w}_1 \mathbf{w}_1^T + k_2 \mathbf{w}_2 \mathbf{w}_2^T + \cdots + k_n \mathbf{w}_n \mathbf{w}_n^T, \tag{5}$$

where $k_i \geq 0$ is the spring stiffness associated with spring wrench $\mathbf{w}_i$.

Now consider a fully serial mechanism consisting of n elastic revolute joints. For a joint J, the unit twist $\mathbf{t}$ centered at the joint is defined as its *joint twist*. In Plücker axis coordinates, joint twist $\mathbf{t}$ has the form:

$$\mathbf{t} = \begin{bmatrix} \mathbf{v} \\ 1 \end{bmatrix}, \tag{6}$$

where $\mathbf{v} = \mathbf{r} \times \mathbf{k}$, $\mathbf{k}$ is the unit vector orthogonal to the plane, and $\mathbf{r}$ is the position vector of the revolute joint with respect to the coordinate frame. The 2-vectors $\mathbf{r}$ and $\mathbf{v}$ (the translational component of $\mathbf{t}$) are related by:

$$\mathbf{r} = \boldsymbol{\Omega} \mathbf{v}, \tag{7}$$

where $\boldsymbol{\Omega}$ is the 2×2 skew-symmetric matrix defined as:

$$\boldsymbol{\Omega} = \begin{bmatrix} 0 & -1 \\ 1 & 0 \end{bmatrix}. \tag{8}$$

https://doi.org/10.1017/S0263574722001448 Published online by Cambridge University Press

Conversely, a unit twist $\mathbf{t}$ in the form of Eq. (6) can be used to represent the location of a point in the plane.

If a compliance matrix $\mathbf{C}$ is passively realized with a serial mechanism having n joints described by joint twists $\mathbf{t}_i$, $(1, \ldots, n)$, then [33]

$$\mathbf{C} = c_1\mathbf{t}_1\mathbf{t}_1^T + c_2\mathbf{t}_2\mathbf{t}_2^T + \cdots + c_n\mathbf{t}_n\mathbf{t}_n^T, \tag{9}$$

where $c_i \geq 0$ is the joint compliance at the joint associated with $\mathbf{t}_i$.

2.3. Compliance of multi-serial mechanisms

As shown in Fig. 2, a compliant hand can be viewed as parallel system in which each finger is a serial mechanism. For an m-serial mechanism, if each $\mathbf{C}_i$ (calculated using Eq. (9)) is the compliance matrix attained at the elastically suspended body by the ith serial mechanism, then the overall Cartesian stiffness of the multi-serial system is

$$\mathbf{K} = \mathbf{C}_1^{-1} + \mathbf{C}_2^{-1} + \cdots + \mathbf{C}_m^{-1}. \tag{10}$$

However, for the compliant hand illustrated in Fig. 2(b), because the fingertip in contact with the object surface is modeled as a free joint (each finger only exerts pure force (no torque) to the body), the planar compliance provided by each finger is rank deficient. In other words, each finger provides only point planar compliance (a 2×2 matrix) rather than general planar compliance (a 3×3 matrix). As such, Eq. (10) cannot be directly applied to a hand as modeled in Fig. 2(b). A different approach to determine the Cartesian stiffness of a hand needs to be developed, as described in the next section.

3. Point planar stiffness and point planar compliance

In this section, the analysis and synthesis of a point planar compliance are presented. Since spring wrenches in a parallel mechanism and joint twists in a serial mechanism are represented by planar screws (3-vectors), the relationship between a 2×2 point stiffness/compliance matrix in $E(2)$ and its 3×3 representation in $SE(2)$ is first presented. Then, the realization of a point planar compliance with both a parallel mechanism and a serial mechanism is addressed.

3.1. Properties of point stiffness and compliance

Consider a 2-spring parallel mechanism having spring wrenches $(\mathbf{w}_1, \mathbf{w}_2)$ and spring rates (k_1, k_2). The stiffness of the 2-spring system is

$$\mathbf{K} = k_1\mathbf{w}_1\mathbf{w}_1^T + k_2\mathbf{w}_2\mathbf{w}_2^T = \begin{bmatrix} \mathbf{K}_t & \mathbf{b} \\ \mathbf{b}^T & k_r \end{bmatrix}, \tag{11}$$

which is a 3×3 rank-2 PSD matrix.

Suppose $\mathbf{w}_1$ and $\mathbf{w}_2$ intersect at point P (Fig. 3), then P must be the stiffness center of $\mathbf{K}$. If the coordinate frame is located at P, the stiffness matrix has the form:

$$\mathbf{K} = \begin{bmatrix} \mathbf{K}_P & \mathbf{0} \\ \mathbf{0} & 0 \end{bmatrix}, \tag{12}$$

where $\mathbf{K}_P$ is a 2×2 PD matrix. Thus, $\mathbf{K}$ is a point stiffness at P. Since the leading 2×2 diagonal block in the stiffness matrix $\mathbf{K}$ is invariant under coordinate translation, $\mathbf{K}_t = \mathbf{K}_P$. As a consequence, the 2×2 translational matrix $\mathbf{K}_P$ can be obtained from the leading block of the 3×3 stiffness $\mathbf{K}$ in *any* coordinate frame. Conversely, it can be proved that any point stiffness in the form of Eq. (12) is readily realized with 2 springs intersecting at the coordinate frame origin. Therefore, to achieve a point stiffness at a location, only the geometry and the elastic properties of two springs intersecting at that location need

https://doi.org/10.1017/S0263574722001448 Published online by Cambridge University Press

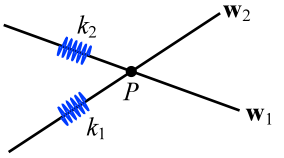

Figure 3. *Any point planar stiffness at point P can be achieved by 2 springs intersecting at P.*

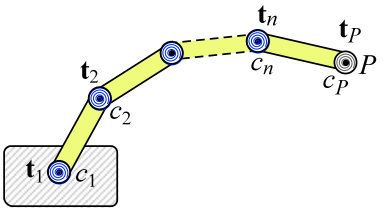

Figure 4. *A point stiffness achieved by a serial mechanism. A free revolute joint is located at the point of interest.*

to be determined. Also, note that not every rank-2 planar 3×3 stiffness matrix can be expressed in the form of Eq. (12), that is, not every rank-2 matrix represents a point stiffness. For example, the stiffness matrix

$$\mathbf{K} = \begin{bmatrix} 1 & 0 & 0 \\ 0 & 0 & 0 \\ 0 & 0 & 1 \end{bmatrix} \tag{13}$$

does not represent a point planar matrix. Although $\mathbf{K}$ in Eq. (13) is a rank-2 PSD matrix, the leading 2×2 block is not full rank and the matrix cannot be realized by two springs intersecting at a point.

In summary, for the planar case, we have

Proposition 1. *A rank-2 stiffness matrix* $\mathbf{K}$ *represents a point planar stiffness at some point if and only if*

(a) *the leading* 2×2 *diagonal block is full rank; or equivalently,*

(b) $\mathbf{K}$ *can be realized by two non-parallel line springs.*

Now consider a serial mechanism (Fig. 4) having n elastic revolute joints described by joint twists $(\mathbf{t}_1, \mathbf{t}_2, \ldots, \mathbf{t}_n)$ with $n \geq 3$. Then, the 3×3 compliance matrix associated with the serial mechanism using Eq. (9) is

$$\mathbf{C}_e = c_1 \mathbf{t}_1 \mathbf{t}_1^T + c_2 \mathbf{t}_2 \mathbf{t}_2^T + \cdots + c_n \mathbf{t}_n \mathbf{t}_n^T. \tag{14}$$

If another joint J_P with compliance c_P is added at the distal link endpoint P, then

$$\mathbf{C} = \mathbf{C}_e + c_P \mathbf{t}_P \mathbf{t}_P^T, \tag{15}$$

where $\mathbf{t}_P$ is the joint twist associated with J_P. When the coordinate frame is located at point P, $\mathbf{t}_P$ is

$$\mathbf{t}_P = \begin{bmatrix} \mathbf{0} \\ 1 \end{bmatrix}. \tag{16}$$

Any full-rank compliance $\mathbf{C}_e$ described at the same coordinate frame has the form

$$\mathbf{C}_e = \begin{bmatrix} \mathbf{C}_P & \mathbf{g} \\ \mathbf{g}^T & c_r \end{bmatrix}. \tag{17}$$

https://doi.org/10.1017/S0263574722001448 Published online by Cambridge University Press

Using Eqs. (15)-(17), the total compliance at P is

$$\mathbf{C} = \begin{bmatrix} \mathbf{C}_P & \mathbf{g} \\ \mathbf{g}^T & c_r + c_p \end{bmatrix}. \tag{18}$$

The location of its compliance center relative to endpoint P is calculated to be:

$$\mathbf{r}_c = -\frac{1}{(c_r + c_p)} \mathbf{\Omega g}, \tag{19}$$

where $\mathbf{\Omega}$ is the skew-symmetric matrix defined in Eq. (8). The inverse of $\mathbf{C}$, the 3×3 stiffness matrix $\mathbf{K}$, is

$$\mathbf{K} = \mathbf{C}^{-1} = \begin{bmatrix} \left(\mathbf{C}_P - \frac{1}{(c_r + c_p)} \mathbf{g}\mathbf{g}^T \right)^{-1} & -\frac{1}{h} \mathbf{C}_P^{-1} \mathbf{g} \\ -\frac{1}{h} \mathbf{g}^T \mathbf{C}_P^{-1} & \frac{1}{h} \end{bmatrix}, \tag{20}$$

where $h = (c_r + c_p) - \mathbf{g}^T \mathbf{C}_P^{-1} \mathbf{g}$.

If $c_p \to +\infty$, then $\mathbf{r}_c \to \mathbf{0}$, meaning that the compliance center is located at P, and the associated stiffness matrix in $SE(2)$ is

$$\mathbf{K} = \begin{bmatrix} \mathbf{C}_P^{-1} & \mathbf{0} \\ \mathbf{0} & 0 \end{bmatrix} = \begin{bmatrix} \mathbf{K}_P & \mathbf{0} \\ \mathbf{0} & 0 \end{bmatrix}. \tag{21}$$

Thus, a point compliance is achieved by placing a free revolute joint at the end of the serial chain at the point of interest. The 2×2 point compliance is the leading 2×2 block in the compliance matrix of the fully elastic serial mechanism. Note that, unlike the stiffness matrix, the leading 2×2 block matrix in the compliance matrix $\mathbf{C}$ associated with an elastic serial mechanism is not invariant under coordinate translation. The point compliance $\mathbf{C}_P$ can be obtained from the 3×3 planar compliance matrix $\mathbf{C}$ *only if* it is expressed at a coordinate frame located at P. Also, to obtain a full-rank point planar compliance, the elastic joints cannot be collinear. This is because, if all joints are located on the same line, any two of the translational components $\mathbf{v}_i$ and $\mathbf{v}_j$ in joint twists $\mathbf{t}_i$ and $\mathbf{t}_j$ must be linearly dependent, making $\mathbf{C}_P$ in Eq. (18) rank deficient (rank 1). In summary,

Proposition 2. *A serial mechanism with elastic joints J_i can achieve a point compliance by adding a free revolute joint at the serial chain endpoint if and only if*

(a) *the number of elastic joints $n \geq 2$; and*

(b) *the locations of all elastic joints are not collinear.*

3.2. Realization of a point compliance

For a point stiffness at a given location, since only force and translation are considered, the force-deflection relation can be expressed as

$$\mathbf{f} = \mathbf{K}_P \mathbf{v}, \tag{22}$$

where the force $\mathbf{f}$ and the displacement $\mathbf{v}$ (the translational component of the twist) are 2-vectors. This relationship can be alternatively expressed as:

$$\mathbf{v} = \mathbf{C}_P \mathbf{f}, \tag{23}$$

where $\mathbf{C}_P = \mathbf{K}_P^{-1}$ is the point compliance at P.

Consider a serial mechanism having n elastic joints, and the point compliance $\mathbf{C}_P$ is at the most distal link tip P. If $\mathbf{r}_i$ is the 2-vector indicating the location of joint J_i relative to the coordinate frame Pxy, then, using Eq. (7), the translational component of the joint twist $\mathbf{t}_i$ is

$$\mathbf{v}_i = \mathbf{\Omega}^T \mathbf{r}_i. \tag{24}$$

https://doi.org/10.1017/S0263574722001448 Published online by Cambridge University Press

If c_i is the joint compliance at J_i, then the 2×2 point compliance at P associated with the n-joint mechanism configuration is

$$\mathbf{C}_P = c_1 \mathbf{v}_1 \mathbf{v}_1^T + c_2 \mathbf{v}_2 \mathbf{v}_2^T + \cdot + c_n \mathbf{v}_n \mathbf{v}_n^T. \tag{25}$$

From Proposition 2, the point compliance can be achieved by a fully serial mechanism having $n \geq 2$ elastic joints. To realize a full-rank PD 2×2 point compliance at point P, at least 2 elastic joints are needed. It can be proved that, if for any two joints, a given passive point compliance is expressed as

$$\mathbf{C}_P = c_1 \mathbf{v}_1 \mathbf{v}_1^T + c_2 \mathbf{v}_2 \mathbf{v}_2^T, \tag{26}$$

then both the coefficients c_1 and c_2 must be positive. In fact, if $\mathbf{r}_i$ is the position of joint J_i with respect to P, then using Eq. (24), $\mathbf{r}_i^T \mathbf{v}_i = 0$. Since $\mathbf{C}_P$ is PD,

$$\mathbf{r}_1^T \mathbf{C}_P \mathbf{r}_1 = c_2 \left(\mathbf{r}_1^T \mathbf{v}_2 \right)^2 > 0. \tag{27}$$

Thus, $c_2 > 0$. Similarly, $c_1 > 0$.

This result for 2 joints is not true for 3 joints. As shown in ref. [34], an arbitrary point compliance matrix $\mathbf{C}_P$ can always be expressed in the form of Eq. (25) at any configuration of a 3R serial mechanism, and the 3 coefficients (c_1, c_2, c_3) are uniquely determined by the locations of the three elastic joints. These coefficients, however, are not guaranteed to all be positive. Based on the result for 2 joints, it is readily shown that among the 3 coefficients c_is, at most one is negative. Conditions on the configuration of a 3R serial mechanism that ensure passive realization of a given point compliance are presented in ref. [34].

When synthesizing a point compliance with a finger for which the locations of the base joint and the fingertip contact are determined, an equivalent and easier to use condition is derived below.

Consider a given 2×2 point compliance matrix $\mathbf{C}_P$ at point P. Suppose that a 3R serial mechanism has joints J_1, J_2, and J_3 and suppose that $\mathbf{r}_i$ is the position of J_i relative to point P. Denote ρ_i as the line collinear with position vector $\mathbf{r}_i$ and denote l_i as the line of action of force $\mathbf{f}_i = \mathbf{K}_P \mathbf{v}_i$. At a given configuration, the compliance is expressed as:

$$\mathbf{C}_P = c_1 \mathbf{v}_1 \mathbf{v}_1^T + c_2 \mathbf{v}_2 \mathbf{v}_2^T + + c_3 \mathbf{v}_3 \mathbf{v}_3^T. \tag{28}$$

For an arbitrary permutation (i, j, s) of $\{1, 2, 3\}$, since $\mathbf{r}_s^T \mathbf{v}_s = 0$ and $\mathbf{C}_P \mathbf{f}_s = \mathbf{v}_s$,

$$\mathbf{r}_s^T \mathbf{C}_P \mathbf{f}_s = c_i \left(\mathbf{r}_s^T \mathbf{v}_i \right) \left(\mathbf{v}_i^T \mathbf{f}_s \right) + c_j \left(\mathbf{r}_s^T \mathbf{v}_j \right) \left(\mathbf{v}_j^T \mathbf{f}_s \right) = 0. \tag{29}$$

Thus, c_i and c_j have the same sign if and only if [$\left(\mathbf{r}_s^T \mathbf{v}_i \right) \left(\mathbf{v}_i^T \mathbf{f}_s \right)$] and [$\left(\mathbf{r}_s^T \mathbf{v}_j \right) \left(\mathbf{v}_j^T \mathbf{f}_s \right)$] have different signs. Consider the following two cases.

Case 1: $\left(\mathbf{r}_s^T \mathbf{v}_i \right)$ and $\left(\mathbf{r}_s^T \mathbf{v}_j \right)$ have the same sign. In this case, joints J_i and J_j are on the same side of line ρ_s. Then $\left(\mathbf{v}_i^T \mathbf{f}_s \right)$ and $\left(\mathbf{v}_j^T \mathbf{f}_s \right)$ must have different signs. Thus, J_i and J_j must be separated by l_s.

Case 2: $\left(\mathbf{r}_s^T \mathbf{v}_i \right)$ and $\left(\mathbf{r}_s^T \mathbf{v}_j \right)$ have different signs. In this case, joints J_i and J_j are separated by ρ_s. Then $\left(\mathbf{v}_i^T \mathbf{f}_s \right)$ and $\left(\mathbf{v}_j^T \mathbf{f}_s \right)$ must have the same sign. Thus, J_i and J_j must be on the same side of l_s.

Thus, c_i and c_j have the same sign if and only if joints J_i and J_j are separated by either line l_s or line ρ_s (but not both). Since, of the 3 coefficients (c_1, c_2, c_3), at most one is negative; therefore, if c_i and c_j have the same sign, they must both be positive. In summary,

Proposition 3. *A given point compliance* $\mathbf{C}_P$ *at point P can be passively realized by a* 3*R serial mechanism if and only if for all permutations* (i, j, s) *of* $\{1, 2, 3\}$, *joints* J_i *and* J_j *are separated by only one of the 2 lines* l_s *and* ρ_s *as illustrated in Fig. 5.*

This general result is simplified when the 3-joint locations $\mathbf{r}_i$ are not collinear and the first joint (base joint) location is specified. For a given point compliance $\mathbf{C}_P$ expressed in the form of Eq. (28), the force $\mathbf{f}_1$ associated with translational twist $\mathbf{v}_1$ at joint J_1 is

$$\mathbf{f}_1 = \mathbf{K}_P \mathbf{v}_1. \tag{30}$$

https://doi.org/10.1017/S0263574722001448 Published online by Cambridge University Press

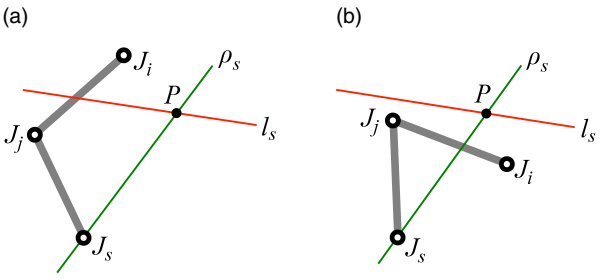

Figure 5. *Necessary and sufficient condition on the joint locations of a 3R mechanism for the realization of a point compliance at a given point P. Joints J_i and J_j must satisfy either: (a) J_i and J_j are separated by line l_s and not by line ρ_s or (b) J_i and J_j are separated by line ρ_s and not by line l_s.*

Then,

$$\mathbf{C}_P\mathbf{f}_1 = c_1\left(\mathbf{v}_1^T\mathbf{f}_1\right)\mathbf{v}_1 + c_2\left(\mathbf{v}_2^T\mathbf{f}_1\right)\mathbf{v}_2 + c_3\left(\mathbf{v}_3^T\mathbf{f}_1\right)\mathbf{v}_3. \tag{31}$$

Since $\mathbf{C}_P\mathbf{f}_1 = \mathbf{v}_1$, if J_3 is located on line l_1 (the line of action of $\mathbf{f}_1$), then $\mathbf{v}_3^T\mathbf{f}_1 = 0$, and Eq. (31) becomes

$$\mathbf{v}_1 = c_1\left(\mathbf{v}_1^T\mathbf{f}_1\right)\mathbf{v}_1 + c_2\left(\mathbf{v}_2^T\mathbf{f}_1\right)\mathbf{v}_2. \tag{32}$$

Since $\mathbf{v}_1$ and $\mathbf{v}_2$ are not collinear, they are linearly independent, and $c_2 = 0$. Thus, if J_3 is located along l_1,

$$\mathbf{C}_P = c_1\mathbf{v}_1\mathbf{v}_1^T + c_3\mathbf{v}_3\mathbf{v}_3^T. \tag{33}$$

As proved in Eqs. (26)-(27), both c_1 and c_3 must be positive regardless of the location of J_2.

Since c_2 changes its sign when J_3 moves across the line of action of $\mathbf{f}_1$, rotation of link L_3 about the fixed point P from a location along $\mathbf{f}_1$ will result in a sign change in c_2. If a rotation yields a location of J_3 such that J_2 and J_3 are separated by either l_1 or ρ_1 (not both), then the 3 coefficients c_1, c_2, and c_3 must all be positive.

In the realization of an arbitrary point compliance using a $3R$ finger with the locations of base joint J_1 and fingertip P specified, only an evaluation of the locations of J_2 and J_3 relative to lines ρ_1 and l_1 is needed. This approach will be used in the synthesis of compliance with multi-finger hands.

4. Compliance realization with a hand

In this section, the realization of an arbitrary compliance with a hand is addressed. The hands considered consist of multiple fingers, each having 3 elastic joints in which the links connecting adjacent finger joints have specified lengths. First, an overview of the synthesis overall approach is presented. Then, procedures used to assess the realizability of a desired elastic behavior are reviewed. The synthesis procedure is then described in detail.

4.1. Approach

Suppose that a specific 3×3 symmetric PD matrix $\mathbf{K}$ is desired for an object grasped by an m-finger hand. To do this, the first step in the synthesis process is to identify a 2m-spring fully parallel mechanism for which pairs of springs intersect on the held object surface at locations P_i. In doing this, the given stiffness is *strategically* decomposed into the sum of rank-2 PSD matrices (each ultimately corresponding to a point planar stiffness provided by a finger). The desired stiffness would then be described by:

$$\mathbf{K} = \mathbf{K}_1 + \mathbf{K}_2 + \ldots + \mathbf{K}_m, \tag{34}$$

where m is the number of fingers in the hand.

https://doi.org/10.1017/S0263574722001448 Published online by Cambridge University Press

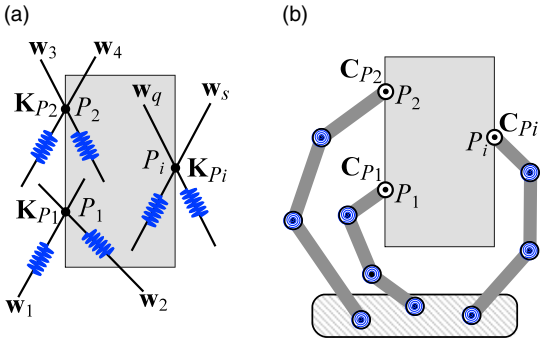

Figure 6. *Realization of an elastic behavior with a multi-finger hand. (a) Realization of the stiffness by a 2m-spring mechanism with each pair of springs intersecting at the object surface. (b) The point compliance* $\mathbf{C}_{Pi} = \mathbf{K}_{Pi}^{-1}$ *associated with each pair of springs is realized by a 3-joint finger.*

In this point stiffness decomposition approach, each $\mathbf{K}_i$ is then realized using the results of Proposition 2 by a 3*R* finger with the fingertip contacting the object surface at point P_i. The *m* fingers together realize the desired $\mathbf{K}$.

Specifically, the approach uses previously developed geometric construction-based synthesis procedures [15, 17] for parallel mechanisms. As such, the decomposition of Eq. (34) is not arbitrary, but strategic. In the process, 2*m* springs are selected with each pair $(\mathbf{w}_q, \mathbf{w}_s)$ intersecting at point P_i on the surface of the object as illustrated in Fig. 6(a). By Proposition 1, the stiffness $\mathbf{K}_i$ associated with $(\mathbf{w}_q, \mathbf{w}_s)$ must be a point stiffness at P_i.

Next, each rank-2 stiffness is converted to a finger compliance matrix at point P_i. Suppose that the 2×2 leading block of $\mathbf{K}_i$ is $\mathbf{K}_{Pi}$, then

$$\mathbf{C}_{Pi} = \mathbf{K}_{Pi}^{-1} \tag{35}$$

is the 2×2 point compliance matrix at P_i to be realized by a finger. Note that $\mathbf{K}_{Pi}$ is expressed in the global coordinate frame *Oxy* and does not change when translated to the frame at P_i, whereas $\mathbf{C}_{Pi}$ obtained from Eq. (35) is the associated point compliance expressed only in the coordinate frame at P_i.

For each point compliance $\mathbf{C}_{Pi}$, one 3-joint finger (a 3*R* serial mechanism) is configured such that the last link contacts the object surface at P_i as shown in Fig. 6(b). As such, the desired compliant behavior is achieved by the grasp.

4.2. Spring distribution constraints

As shown in ref. [20] in order for a parallel mechanism to realize a specified elastic behavior, the locations and orientations of the springs in the mechanism must satisfy a set of necessary conditions. Below, the necessary conditions on the spring distribution of a parallel mechanism are reviewed.

For a given stiffness matrix $\mathbf{K}$, the distribution conditions [20] on the springs in a parallel mechanism for the realization of $\mathbf{K}$ are described by a circle Γ_k centered at the stiffness center C_c and a pair of lines γ^+ and γ^- intersecting at C_c. The circle and the line pair are determined by the principal stiffnesses of the stiffness matrix.

Suppose that k_χ and k_η are the two translational principal stiffnesses along the principal χ- and η-axis, respectively, and k_τ is the rotational principal stiffness of stiffness matrix $\mathbf{K}$. The radius of Γ_k is

$$r_k = \sqrt{\frac{k_\tau}{k_\chi + k_\eta}}. \tag{36}$$

https://doi.org/10.1017/S0263574722001448 Published online by Cambridge University Press

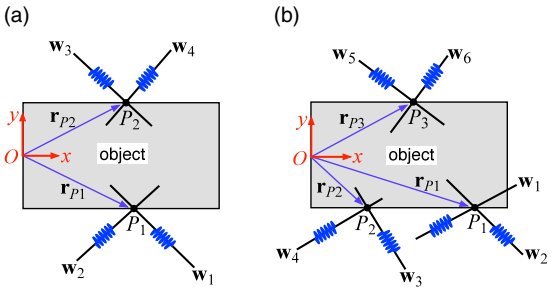

Figure 7. *Realization of the compliant behavior with a 2m-spring parallel mechanism. (a) A 4-spring mechanism. (b) A 6-spring mechanism. For both cases, the intersection of each pair of springs is located at the surface of the object.*

The angles between line γ^+ (γ^-) and the principal χ-axis are

$$\theta = \pm \sin^{-1} \sqrt{\frac{k_\chi}{k_\chi + k_\eta}}. \tag{37}$$

If $\mathbf{r}_i$ is the perpendicular vector from compliance center C_c to the ith spring axis, then the following conditions must be satisfied by the set of springs in the parallel mechanism:

(i) At least one spring line of action intersects Γ_k, and at least one spring line of action does not intersect Γ_k;

(ii) All $\mathbf{r}_i$s span more than a half plane, and at least 2-vectors $\mathbf{r}_i$ and $\mathbf{r}_j$ are separated by either γ^+ or γ^- but not both.

Since the synthesis approach is based on the realization of the compliance with a $2m$-spring parallel mechanism, these necessary conditions should be considered before and while performing the synthesis procedure.

4.3. Synthesis procedure

The more detailed procedure presented below is used to synthesize a given compliant behavior with a multi-finger hand. Each finger has 3 elastic joints and fixed link lengths. In a coordinate frame Oxy, the desired stiffness for the held body is $\mathbf{K}$.

Step 1: Parallel mechanism synthesis

Realize $\mathbf{K}$ with a fully parallel mechanism to obtain the corresponding point compliance matrices at the surface of the object. The desired stiffness is first realized by a $2m$-spring parallel mechanism in which pairs of springs intersect at the object surface. Here, cases for which the number of fingers $m = 2$, $m = 3$, and $m > 3$ are considered.

(i) $m = 2$. Using the process developed in ref. [29], 4-spring wrenches ($\mathbf{w}_1, \mathbf{w}_2, \mathbf{w}_3, \mathbf{w}_4$) and the corresponding spring rates (k_1, k_2, k_3, k_4) are obtained. In the geometry-based spring selection procedure [29], the intersections of ($\mathbf{w}_1, \mathbf{w}_2$) and ($\mathbf{w}_3, \mathbf{w}_4$), P_1 and P_2, are located on the surface of the held object as shown in Fig. 7(a).

The two rank-2 stiffness matrices associated with ($\mathbf{w}_1, \mathbf{w}_2$) and ($\mathbf{w}_3, \mathbf{w}_4$) are

$$\mathbf{K}_1 = k_1 \mathbf{w}_1 \mathbf{w}_1^T + k_2 \mathbf{w}_2 \mathbf{w}_2^T, \tag{38}$$

$$\mathbf{K}_2 = k_3 \mathbf{w}_3 \mathbf{w}_3^T + k_4 \mathbf{w}_4 \mathbf{w}_4^T. \tag{39}$$

https://doi.org/10.1017/S0263574722001448 Published online by Cambridge University Press

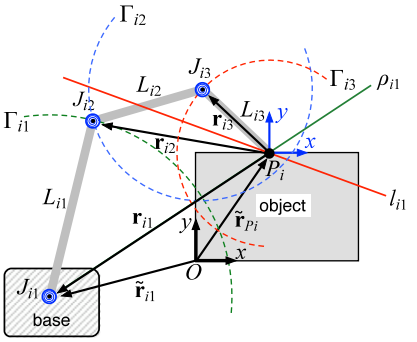

Figure 8. *Realization of point compliance $\mathbf{C}_{Pi}$ by a 3-joint finger having fixed link lengths. The locations of joints J_{i2} and J_{i3} must be separated by line l_{i1} (or ρ_{i1}) and be on the same side of line ρ_{i1} (or l_{i1}).*

The 3×3 planar stiffness matrices $\mathbf{K}_1$ and $\mathbf{K}_2$ are converted to 2×2 point stiffness matrices at P_1 and P_2, $\mathbf{K}_{P1}$ and $\mathbf{K}_{P2}$, by extracting the leading 2×2 blocks of $\mathbf{K}_1$ and $\mathbf{K}_2$, respectively.

The twists associated with fingertip contact points P_1 and P_2 are calculated as

$$\hat{\mathbf{t}}_{P1} = \mathbf{w}_1 \times \mathbf{w}_2, \tag{40}$$

$$\hat{\mathbf{t}}_{P2} = \mathbf{w}_3 \times \mathbf{w}_4, \tag{41}$$

which are each converted to unit twists, $\mathbf{t}_{P1}$ and $\mathbf{t}_{P2}$. The position vectors of P_1 and P_2 in Oxy, $\tilde{\mathbf{r}}_{P1}$ and $\tilde{\mathbf{r}}_{P2}$, are then obtained using Eq. (7):

$$\tilde{\mathbf{r}}_{P1} = \mathbf{\Omega}\mathbf{v}_{P1}, \tag{42}$$

$$\tilde{\mathbf{r}}_{P2} = \mathbf{\Omega}\mathbf{v}_{P2}, \tag{43}$$

where $\mathbf{v}_{P1}$ and $\mathbf{v}_{P2}$ are the first two components of the unit twists $\mathbf{t}_{P1}$ and $\mathbf{t}_{P2}$, respectively, and $\mathbf{\Omega}$ is the matrix defined in Eq. (8).

The two 2×2 point compliance matrices at P_1 and P_2 are then obtained:

$$\mathbf{C}_{P1} = \mathbf{K}_{P1}^{-1}, \quad \mathbf{C}_{P2} = \mathbf{K}_{P2}^{-1}. \tag{44}$$

(ii) $m = 3$. Similarly, using the process presented in ref. [29], 6-spring wrenches $(\mathbf{w}_1, \mathbf{w}_2, \ldots, \mathbf{w}_6)$ and corresponding spring rates $(k_1, k_2, k_3, k_4, k_5, k_6)$ are selected such that pairs of springs wrenches intersect on the object surface. The intersections of $(\mathbf{w}_1, \mathbf{w}_2)$, $(\mathbf{w}_3, \mathbf{w}_4)$, and $(\mathbf{w}_5, \mathbf{w}_6)$ are illustrated in Fig. 7(b).

Following an equivalent process to that described in Eqs. (40)-(44), the 2×2 point compliance matrices $\mathbf{C}_{Pi}$ at P_i $(i = 1, 2, 3)$ and the position vectors $\mathbf{r}_{Pi}$ are obtained.

(iii) $m > 3$. The 3-finger process can be extended to the case $m > 3$. For example, for $m = 4$, first obtain three rank-2 point stiffness matrices $\mathbf{K}_{P1}$, $\mathbf{K}_{P2}$, $\mathbf{K}_{P3}$ on the object surface using the above process for $m = 3$. Then $\mathbf{C}_{P1} = \mathbf{K}_{P1}^{-1}$ can be realized with a 3-joint finger. Let

$$\hat{\mathbf{K}}_2 = \mathbf{K}_{P2} + \mathbf{K}_{P3}.$$

Then, $\hat{\mathbf{K}}_2$ can be realized with three fingers using the 3-finger synthesis process. As such, the desired stiffness is achieved with a hand having a total of 4 fingers by successive use of the 3-finger process.

Step 2: Compliance synthesis for each finger

Synthesis of each $\mathbf{C}_{Pi}$ with a 3-joint finger. For each finger, if both the contact point P_i (determined in Step 1) and the location of the base joint J_{i1} of a finger are specified, the 3-joint finger with fixed lengths is kinematically equivalent to a 4-bar mechanism having link lengths L_{i1}, L_{i2}, and L_{i3} (as shown in Fig. 8).

https://doi.org/10.1017/S0263574722001448 Published online by Cambridge University Press

(i) Express each joint position in a local contact point coordinate frame $P_i xy$. If the location of the base joint J_{i1} in the global coordinate frame Oxy is $\tilde{\mathbf{r}}_{i1}$, then in the coordinate frame $P_i xy$, the position of the base joint is

$$\mathbf{r}_{i1} = \tilde{\mathbf{r}}_{i1} - \tilde{\mathbf{r}}_{Pi}. \tag{45}$$

(ii) Obtain $\mathbf{v}_{i1}$ using Eq. (24), then calculate $\mathbf{f}_{i1} = \mathbf{K}_{Pi}\mathbf{v}_{i1}$ and obtain its line of action l_{i1}.

(iii) Select the position of J_{i3} by rotating link L_{i3} about P_i such that J_{i3} and J_{i2} are separated by l_{i1} and on the same side of ρ_{i1} (alternatively, are separated by ρ_{i1} and on the same side of l_{i1}) as illustrated in Fig. 8.

(iv) Determine the location of J_{i2} using the finger geometry. The joint must be located at the intersection of circle Γ_{i1} of radius L_{i1} centered at J_{i1} and circle Γ_{i2} of radius L_{i2} centered at J_{i3} as shown in Fig. 8.

(v) Calculate the joint compliances using [34]

$$c_1 = \frac{\mathbf{r}_2^T \mathbf{C} \mathbf{r}_3}{\left(\mathbf{r}_2^T \mathbf{v}_1\right)\left(\mathbf{r}_3^T \mathbf{v}_1\right)}, \tag{46}$$

$$c_2 = \frac{\mathbf{r}_3^T \mathbf{C} \mathbf{r}_1}{\left(\mathbf{r}_3^T \mathbf{v}_2\right)\left(\mathbf{r}_1^T \mathbf{v}_2\right)}, \tag{47}$$

$$c_3 = \frac{\mathbf{r}_1^T \mathbf{C} \mathbf{r}_2}{\left(\mathbf{r}_1^T \mathbf{v}_3\right)\left(\mathbf{r}_2^T \mathbf{v}_3\right)}. \tag{48}$$

Step 3: Determination of hand configuration

Obtain each joint location in the global coordinate frame. For finger i, each joint location is calculated using

$$\tilde{\mathbf{r}}_{ij} = \tilde{\mathbf{r}}_{Pi} + \mathbf{r}_{ij}, \quad j = 1, 2, 3. \tag{49}$$

With the final step, all finger configurations and elastic properties are identified.

4.4. Discussion

The synthesis of a grasp stiffness depends on the locations where fingers contact the object, which directly relate to the selection of spring intersections on the object surface. In selecting a set of springs, the spring distribution necessary conditions [20] (reviewed in Section 4.2) need to be considered. It should be noted that the realizability of a stiffness with a given hand depends not only on the given stiffness but also on the shape of the object and the geometry of the hand. Not every stiffness matrix can be realized by a compliant grasp due to the conditions associated with point contact on the object surface. If the compliant behavior cannot be realized by a $2m$-spring parallel mechanism with springs intersecting at the object surface using the results of refs. [15] or [17], then the behavior cannot be achieved by any m-finger compliant hand modeled as shown in Fig. 2(b) regardless of the number of elastic joints or the locations of fingertip contact with the object.

When the desired locations of fingertip contact are identified, each contact point P_i must be in the workspace of a finger so that all contact points can be reached by a given hand. This requirement should be considered in selecting the location of the hand base and in selecting the intersection locations of spring pairs in the first step.

As stated previously, if the contact point and the base joint locations are determined, a 3-joint finger is equivalent to a 4-bar mechanism. The ability of a finger to achieve an arbitrary point compliance depends on its relative link lengths. For example, if the mechanism is Grashof with L_3 being the shortest link, then any point compliance matrix can be realized [34]. Thus, in designing finger geometry, the last link (the one in contact with the object) should be the shortest one. The contact point should not be

https://doi.org/10.1017/S0263574722001448 Published online by Cambridge University Press

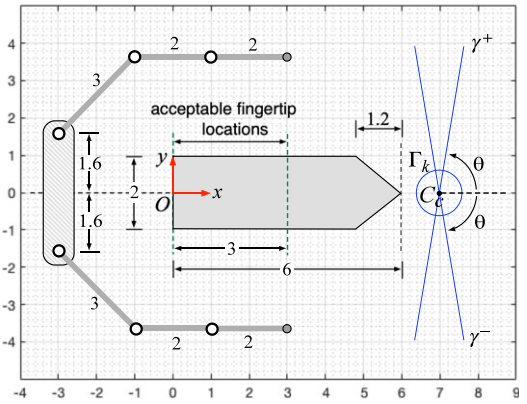

Figure 9. *The dimension of a given object, the location of the base (palm), and geometry of a given 2-finger hand used to realize the desired compliance.*

close to the boundary of the finger workspace so that it has sufficient mobility to vary the locations of the other joints in order to achieve the desired point compliance.

Hard fingertip contact with the surface of a held object is modeled as a free revolute joint. This model is based on the assumption that the fingertip does not slip on the object surface. This requires that friction between the fingertip and the object surface is sufficient to prevent slipping. If slipping does occur, force closure from all fingertips of a hand cannot be established, and a stable grasp cannot be accomplished. The theory presented in this paper is valid only for non-slip cases. In the synthesis process, the locations of fingertip contact points should be judiciously selected so that force closure and a stable grasp can be achieved for a desired full-rank compliance matrix.

5. Example

In this section, an example is provided to illustrate the synthesis procedures. The realization of a desired compliance is described in detail for a 2-finger hand. The extension of the synthesis procedure for a 3-finger hand is summarized.

The compliance to be realized by a hand is one obtained from optimizing the object compliance for a peg-in-hole assembly problem [35]. The held body is a stake with the geometry illustrated in Fig. 9. In the coordinate frame Oxy shown at the left side of the stake, the desired compliance is

$$\mathbf{C} = \begin{bmatrix} 0.03 & 0.00 & 0.00 \\ 0.00 & 5.00 & -0.56 \\ 0.00 & -0.56 & 0.08 \end{bmatrix}. \tag{50}$$

The stiffness matrix is

$$\mathbf{K} = \mathbf{C}^{-1} = \begin{bmatrix} 33.3333 & 0 & 0 \\ 0 & 0.9259 & 6.4815 \\ 0 & 6.4815 & 57.8704 \end{bmatrix}. \tag{51}$$

The compliance center C_c is calculated to be at $(7, 0)$. The acceptable fingertip contact locations are selected to be in the range $(0 < x < 3)$ on the opposing edges of the stake as shown in Fig. 9.

As described in Section 4.2, a set of necessary conditions on the locations and orientations of the springs in the mechanism must be satisfied. These conditions should be evaluated before performing the synthesis procedure. Below, the set of necessary conditions on the spring distribution of a parallel mechanism is evaluated for the given stiffness matrix and object.

https://doi.org/10.1017/S0263574722001448 Published online by Cambridge University Press

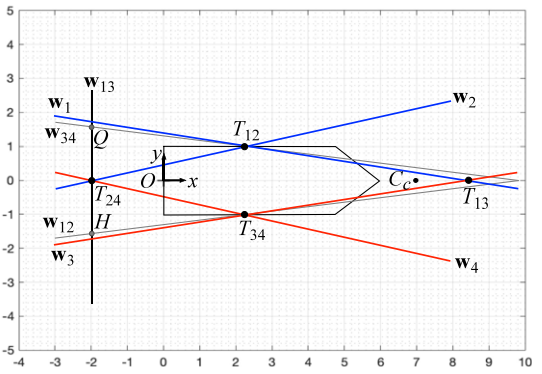

Figure 10. *Compliance synthesis with a 4-spring parallel mechanism. The intersections of spring pairs* $(\mathbf{w}_1, \mathbf{w}_2)$ *and* $(\mathbf{w}_3, \mathbf{w}_4)$ *will be the contact locations of the two fingertips.*

5.1. Distribution condition evaluation

The two necessary conditions on the parallel spring distribution described in Section 4.2 are evaluated for the given stiffness matrix $\mathbf{K}$ (in Eq. (51)) and the object.

The three principal stiffnesses of $\mathbf{K}$ are

$$[k_\chi, k_\eta, k_\tau] = [33.3333, 0.9259, 12.5000],$$

and the principal axes are parallel to the coordinate frame axes. The radius of circle Γ_k is calculated using Eq. (36) to be:

$$r_k = 0.6040.$$

The angles between line γ^+ is calculated using Eq. (37) as:

$$\theta = 80.5377^\circ.$$

Circle Γ_k and lines $\gamma^\pm$ are illustrated in Fig. 9. Since Γ_k does not enclose the peg, a set of $2m$ springs can be selected to meet the two distribution conditions, where m is the number of fingers eventually used in the realization.

5.2. Compliance synthesis with a 2-finger hand

The desired compliance is first realized with a 4-spring parallel mechanism with pairs of springs intersecting at locations within the acceptable area on the body surface ($x < 3$ shown in Fig. 9). Then, each point compliance associated with the intersecting spring pairs is synthesized with a 3-joint finger.

Step 1: Stiffness synthesis with a parallel mechanism

A 4-spring parallel mechanism synthesis procedure is used to obtain the two locations of fingertip contact with the body surface. The fingertip contact points are at the two locations where spring pairs intersect. A procedure similar to that presented in ref. [29] is used. The geometry associated with each step is illustrated in Fig. 10.

1. Choose point T_{12} (where spring wrenches $\mathbf{w}_1$ and $\mathbf{w}_2$ intersect) and point T_{34} (where spring wrenches $\mathbf{w}_3$ and $\mathbf{w}_4$ intersect) on the body surface with $x < 3$. For a selected location of T_{12} represented by twist $\mathbf{t}_{12}$, calculate the corresponding wrench:

$$\mathbf{w}_{12} = \mathbf{K}\mathbf{t}_{12}.$$

The axis of $\mathbf{w}_{12}$ must intersect the opposite edge of the stake in the acceptable range $x < 3$; otherwise, the given compliant behavior cannot be realized. The location of the intersection of

https://doi.org/10.1017/S0263574722001448 Published online by Cambridge University Press

the second spring pair, T_{34}, is at the intersection of $\mathbf{w}_{12}$ and the edge on the opposite side of the stake.

Note that when T_{12} varies along the body edge, T_{34} varies along the opposite edge. Here, the location of T_{12} is chosen such that T_{34} has the same x-coordinate. For the given problem, this is possible and the two points can be determined by the following step.

Let $\mathbf{t}_{12} = [1, -x, 1]^T$ be the twist associated with T_{12}, then if T_{34} has the same horizontal coordinate x, the corresponding twist $\mathbf{t}_{34} = [-1, -x, 1]^T$. The value of x is determined by

$$\mathbf{t}_{34}^T \mathbf{K} \mathbf{t}_{12} = 0$$

which yields $x = 2.2566$. Thus, points (2.2566, 1) and (2.2566, −1) are selected as the locations of T_{12} and T_{34}. These two points will be the fingertip contact locations, P_1 and P_2.

Calculate the wrenches associated with T_{12} and T_{34}: $\hat{\mathbf{w}}_{12} = \mathbf{K}\mathbf{t}_{12}$ and $\hat{\mathbf{w}}_{34} = \mathbf{K}\mathbf{t}_{34}$. The normalized two unit wrenches are

$$\mathbf{w}_{12} = [0.9914, 0.1306, 1.2862]^T,$$

$$\mathbf{w}_{34} = [-0.9914, 0.1306, 1.2862]^T.$$

2. Select wrench $\mathbf{w}_{13}$. Here, a vertical line passing through point $(-2, 0)$ is selected as the line of action of $\mathbf{w}_{13}$ in order to project $\mathbf{t}_{13}$ on the far side of C_c so that the distribution conditions can be satisfied. Then,

$$\mathbf{w}_{13} = [0, -1, 2]^T,$$

which intersects $\mathbf{w}_{12}$ and $\mathbf{w}_{34}$ at H and Q, respectively, as shown in Fig. 10. Calculate the corresponding twist:

$$\mathbf{t}_{13} = \mathbf{C}\mathbf{w}_{13} = [0, -6.1200, 0.7200]^T.$$

The center of $\mathbf{t}_{13}$, T_{13}, is determined to be $(8.5, 0)$.

3. Select the location of T_{24} on the axis of $\mathbf{w}_{13}$ between H and Q. This point is selected to be $(-2, 0)$ for the spring layout to be symmetric about the x-axis. The twist associated with T_{24} is

$$\mathbf{t}_{24} = [0, 2, 1]^T.$$

4. Determine the 4-spring axes. The 4-spring axes can be determined by

$$\hat{\mathbf{w}}_i = \mathbf{t}_{ij} \times \mathbf{t}_{im}.$$

The 4 normalized spring wrenches are

$$[\mathbf{w}_1, \mathbf{w}_2, \mathbf{w}_3, \mathbf{w}_4] = \begin{bmatrix} 0.9874 & -0.9735 & 0.9874 & -0.9735 \\ -0.1582 & -0.2287 & 0.1582 & 0.2287 \\ -1.3443 & 0.4574 & 1.3443 & -0.4574 \end{bmatrix}.$$

Once the 4-spring wrenches are determined, the corresponding spring rates can be obtained using the equations developed in [15]. The calculated spring rates are

$$[k_1, k_2, k_3, k_4] = [15.8652, 1.2645, 15.8652, 1.2645].$$

The axes of the 4 springs are illustrated in Fig. 10.

5. Obtain the two 3×3 stiffness matrices described at Oxy associated with the spring pair intersections at T_{12} and T_{34}:

$$\mathbf{K}_1 = k_1 \mathbf{w}_1 \mathbf{w}_1^T + k_2 \mathbf{w}_2 \mathbf{w}_2^T = \begin{bmatrix} 16.6667 & -2.1960 & -21.6222 \\ -2.1960 & 0.4630 & 3.2407 \\ -21.6222 & 3.2407 & 28.9352 \end{bmatrix},$$

https://doi.org/10.1017/S0263574722001448 Published online by Cambridge University Press

$$\mathbf{K}_2 = k_3\mathbf{w}_3\mathbf{w}_3^T + k_4\mathbf{w}_4\mathbf{w}_4^T = \begin{bmatrix} 16.6667 & 2.1960 & 21.6222 \\ 2.1960 & 0.4630 & 3.2407 \\ 21.6222 & 3.2407 & 28.9352 \end{bmatrix}.$$

The 2×2 point stiffness matrices are obtained by extracting the 2×2 leading blocks for $\mathbf{K}_1$ and $\mathbf{K}_2$:

$$\mathbf{K}_{P1} = \begin{bmatrix} 16.6667 & -2.1960 \\ -2.1960 & 0.4630 \end{bmatrix},$$

$$\mathbf{K}_{P2} = \begin{bmatrix} 16.6667 & 2.1960 \\ 2.1960 & 0.4630 \end{bmatrix}.$$

The two point compliance matrices at points T_{12} and T_{34} are then obtained by taking the inverse of $\mathbf{K}_{P1}$ and $\mathbf{K}_{P2}$:

$$\mathbf{C}_{P1} = \begin{bmatrix} 0.1600 & 0.7589 \\ 0.7589 & 5.7600 \end{bmatrix},$$

$$\mathbf{C}_{P2} = \begin{bmatrix} 0.1600 & -0.7589 \\ -0.7589 & 5.7600 \end{bmatrix}.$$

Step 2: Compliance synthesis for each finger

The desired compliance is realized with the 2-finger hand by identifying the joint stiffnesses and the configuration of each finger. In the following, only the synthesis for one finger ($\mathbf{C}_{P1}$ at P_1) is presented.

Since the base joint J_{11} location (given in the base location and geometry) and the finger tip P_1 location (calculated in Step 1) are determined, only the locations of the second and third joints J_{12} and J_{13} need to be identified.

In the local coordinate frame P_1xy, the position vector (using Eq. (45)) and the corresponding translational twist of base joint J_{11} are

$$\mathbf{r}_{11} = [-5.2566, 0.6]^T, \quad \mathbf{v}_{11} = [0.6, 5.2566]^T.$$

The locations of J_{12} and J_{13} can be identified by the following procedure. The geometry associated with each step is illustrated in Fig. 11(a).

1. Calculate force $\mathbf{f}_{11}$ associated with joint twist $\mathbf{v}_{11}$:

$$\mathbf{f}_{11} = \mathbf{K}_{P1}\mathbf{v}_{11} = [-1.5436, 1.1160]^T.$$

   The line of action of $\mathbf{f}_{11}$, l_{11}, obtained is shown in Fig. 11(a).

2. Select the location of J_{13}. Joint J_{13} must be on circle Γ_3 of radius L_3 centered at P_1. Here, in the local frame P_1xy, $\mathbf{r}_{13}$ is arbitrarily selected to be:

$$\mathbf{r}_{13} = L_3[-\cos 25^\circ, \sin 25^\circ]^T = [-1.8126, 0.8452]^T.$$

3. Determine the location of J_{12}. Once J_{13} is selected, joint J_{12} must be located at the intersection of circles Γ_{11} and Γ_{12} with radii L_1 and L_2 and centered at J_{11} and J_{13}, respectively. There are two intersection points J_{12} and J'_{12}. Both are acceptable in that each is separated from J_{13} by either ρ_{11} or l_{11}, but not both. The one that is separated from J_{13} by l_{11} is chosen. This joint location is determined to be:

$$\mathbf{r}_{12} = [-2.9353, 2.5004]^T.$$

https://doi.org/10.1017/S0263574722001448 Published online by Cambridge University Press

Table I. *Finger joint locations and joint compliances for the obtained hand configuration.*

Finger	Joint	Location	Joint compliance
1	1	(−3.0000, 1.6000)	0.2017
	2	(−0.6787, 3.5004)	0.0106
	3	(0.4440, 1.8452)	0.0293
2	1	(−3.0000, −1.6000)	0.2017
	2	(−0.6787, −3.5004)	0.0106
	3	(0.4440, −1.8452)	0.0293

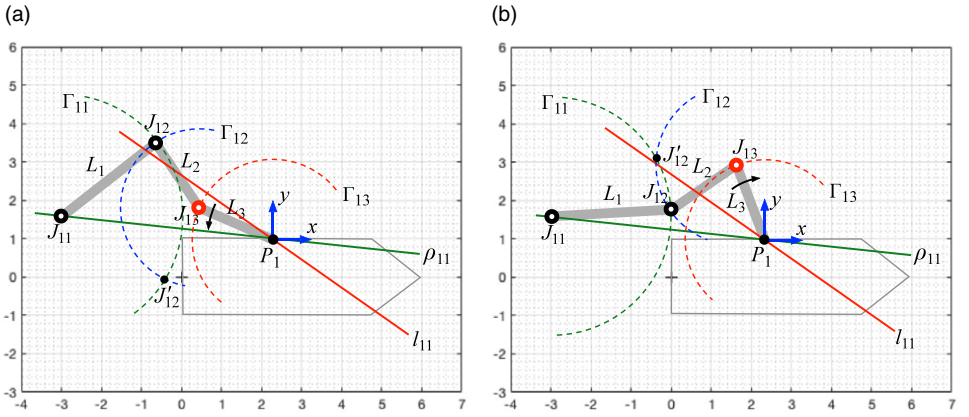

Figure 11. *Synthesis of point compliance at P_1 with a finger of a given hand. Each of the following two approaches yields an acceptable joint configuration. (a) Rotate L_3 about P_1 (counterclockwise) such that J_{13} and J_{12} are separated by line l_{11}. (b) Rotate L_3 about P_1 (clockwise) such that J_{13} and J_{12} are separated by line l_{11}.*

The translational components of the joint twists associated with the selected joints are

$$[\mathbf{v}_{11}, \mathbf{v}_{12}, \mathbf{v}_{13}] = \begin{bmatrix} -0.6000 & -2.5004 & -0.8452 \\ -5.2566 & -2.9353 & -1.8126 \end{bmatrix}.$$

4. Calculate the joint compliances using Eqs. (46)-(48):

$$[c_{11}, c_{12}, c_{13}] = [0.2017, 0.0106, 0.0293].$$

With this final step, a finger to achieve the point compliance $\mathbf{C}_{P1}$ is obtained. The joint locations of J_{12} and J_{13} in the original coordinate frame Oxy are determined using Eq. (49) to be:

$$\tilde{\mathbf{r}}_{12} = [-0.6787, 3.5004]^T,$$

$$\tilde{\mathbf{r}}_{13} = [0.4440, 1.8452]^T.$$

The 3-joint locations in the original coordinate frame Oxy and the values of corresponding joint compliances are listed in Table I.

Alternatively, joint J_{13} could have been selected to be on the other side of line l_{11} by rotating L_3 clockwise (as shown in Fig. 11(b)). If J_{13} is arbitrarily selected as:

$$\mathbf{r}_{13} = L_3[-\cos 70^\circ, \sin 70^\circ]^T = [-0.6840, 1.8794]^T,$$

then, the two intersection points of circles Γ_1 and Γ_2 are located at J_{12} and J'_{12} as illustrated in Fig. 11(b).

Only J_{12} is separated by l_{11} from J_{13} which is located at:

$$\mathbf{r}_{12} = [-2.2569, 0.6440]^T.$$

https://doi.org/10.1017/S0263574722001448 Published online by Cambridge University Press

Table II. *Finger joint locations and joint compliances for the alternative hand configuration.*

Finger	Joint	Location	Joint compliance
1	1	(−3.0000, 1.6000)	0.1906
	2	(−0.0003, 1.6440)	0.0957
	3	(1.5725, 2.8794)	0.0146
2	1	(−3.0000, −1.6000)	0.1906
	2	(−0.0003, −1.6440)	0.0957
	3	(1.5725, −2.8794)	0.0146

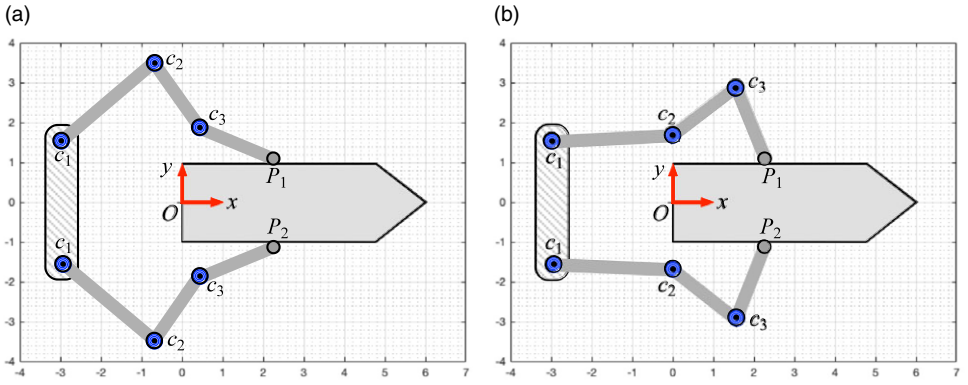

Figure 12. *Compliance synthesis with a 2-finger hand. The desired compliance can be achieved by the same hand at different symmetric configurations (a) and (b) with different joint stiffnesses.*

Then, the 3 alternative joint locations are determined. The 3-joint twists are

$$[\mathbf{v}_{11}, \mathbf{v}_{12}, \mathbf{v}_{13}] = \begin{bmatrix} -0.6000 & -0.6440 & -1.8794 \\ -5.2566 & -2.2569 & -0.6840 \end{bmatrix}.$$

The 3-joint compliances are calculated using Eqs. (46)-(48):

$$[c_{11}, c_{12}, c_{13}] = [0.1906, 0.0957, 0.0146].$$

The alternative locations of J_{12} and J_{13} in the original coordinate frame Oxy are

$$\tilde{\mathbf{r}}_{12} = [-0.0003, 1.6440]^T,$$
$$\tilde{\mathbf{r}}_{13} = [1.5725, 2.8794]^T.$$

The 3-joint locations in the original coordinate frame Oxy and the values of corresponding joint compliances for the alternative hand configuration are listed in Table II.

Using the same process, point compliance $\mathbf{C}_{P2}$ at point P_2 can be achieved by the second finger. Since the compliant behavior is symmetric about the x-axis along the peg's symmetric axis, one can choose the finger configuration symmetric about the axis with the same joint compliances. Figure 12(a) and (b) illustrates the two selected symmetric hand configurations that realize the desired compliance. Note that, due to kinematic redundancy and the ability to select each joint compliance using variable stiffness actuation, there are infinitely many other possible configurations that realize the desired elastic behavior.

https://doi.org/10.1017/S0263574722001448 Published online by Cambridge University Press

5.3. Result verification

For the hand configuration shown in Fig. 12(a), the 2×2 point compliance matrices at the fingertip P_1 are calculated using the joint compliances and joint twists obtained in the procedure.

$$\mathbf{C}_{P1} = c_{11}\mathbf{v}_{11}\mathbf{v}_{11}^T + c_{12}\mathbf{v}_{12}\mathbf{v}_{12}^T + c_{13}\mathbf{v}_{13}\mathbf{v}_{13}^T = \begin{bmatrix} 0.1600 & 0.7589 \\ 0.7589 & 5.7600 \end{bmatrix}.$$

The joint translational twists associated with the symmetric finger configuration at P_2 in Fig. 12(a) are

$$[\mathbf{v}_{11}, \mathbf{v}_{12}, \mathbf{v}_{13}] = \begin{bmatrix} 0.6000 & 2.5004 & 0.8452 \\ -5.2566 & -2.9353 & -1.8126 \end{bmatrix}.$$

The associated point compliance is

$$\mathbf{C}_{P2} = c_{21}\mathbf{v}_{21}\mathbf{v}_{21}^T + c_{22}\mathbf{v}_{22}\mathbf{v}_{22}^T + c_{23}\mathbf{v}_{23}\mathbf{v}_{23}^T = \begin{bmatrix} 0.1600 & -0.7589 \\ -0.7589 & 5.7600 \end{bmatrix}.$$

The 3×3 stiffness matrices in the local coordinate frames at P_1 and P_2 are

$$\tilde{\mathbf{K}}_{P1} = \begin{bmatrix} \mathbf{C}_{P1}^{-1} & \mathbf{0} \\ \mathbf{0} & 0 \end{bmatrix} = \begin{bmatrix} 16.6667 & -2.1960 & 0 \\ -2.1960 & 0.4630 & 0 \\ 0 & 0 & 0 \end{bmatrix},$$

$$\tilde{\mathbf{K}}_{P2} = \begin{bmatrix} \mathbf{C}_{P2}^{-1} & \mathbf{0} \\ \mathbf{0} & 0 \end{bmatrix} = \begin{bmatrix} 16.6667 & 2.1960 & 0 \\ 2.1960 & 0.4630 & 0 \\ 0 & 0 & 0 \end{bmatrix}.$$

The transformation (translation) matrices from local coordinate frames P_1xy and P_2xy to the original frame Oxy, respectively, are

$$\mathbf{T}_{P1} = \begin{bmatrix} 1 & 0 & 1 \\ 0 & 1 & -2.2566 \\ 0 & 0 & 1 \end{bmatrix}, \mathbf{T}_{P2} = \begin{bmatrix} 1 & 0 & -1 \\ 0 & 1 & -2.2566 \\ 0 & 0 & 1 \end{bmatrix}.$$

In the original coordinate frame, the grasp stiffness matrix of the 2-finger hand is

$$\mathbf{K}_h = \mathbf{T}_{P1}^T\tilde{\mathbf{K}}_{P1}\mathbf{T}_{P1} + \mathbf{T}_{P2}^T\tilde{\mathbf{K}}_{P2}\mathbf{T}_{P2} = \begin{bmatrix} 33.3333 & 0 & 0 \\ 0 & 0.9259 & 6.4815 \\ 0 & 6.4815 & 57.8704 \end{bmatrix},$$

which confirms that the desired stiffness matrix in Eq. (51) is achieved.

Using the same process, it is also verified that the hand configuration in Fig. 12(b) realizes the desired elastic behavior.

5.4. Compliance synthesis with a hand having 3 or more fingers

The desired compliant behavior can be also realized with a hand having 3 or more joints. Similar to the process used for a 2-finger hand, the desired behavior is first realized with a 6-spring parallel mechanism with spring pairs intersecting at the surface of the peg and the corresponding point compliance matrix at each contact point is obtained. Then, each point compliance is realized with a finger of the hand.

If use of more fingers is desired, as discussed in Section 4.3, the synthesis procedures for 2-finger and 3-finger hands can be used to decompose the given stiffness matrix into the sum of m rank-2 point stiffness matrices $\mathbf{K}_{Pi}$. Then, using the process (Step 2) described in Section 4.3, each $\mathbf{K}_{Pi}$ is achieved by a 3-joint finger.

https://doi.org/10.1017/S0263574722001448 Published online by Cambridge University Press

6. Summary

In this paper, an approach to providing an object an arbitrary compliance with a compliant hand is developed. The hands considered in this paper have multiple fingers for which each has 3 modulated joint stiffnesses and predetermined link lengths.

Synthesis procedures for 2-finger, 3-finger, and more than 3-finger hands are described. Using these results, any given hand having the corresponding topology can achieve a large space of compliant behaviors by adjusting the joint compliances of each finger and by changing the locations of fingertip contact on the surface of the held object.

If the compliant behavior cannot be achieved by a $2m$-spring parallel mechanism with spring pairs intersecting at the object surface, then the behavior cannot be realized by any m-finger compliant hand as modeled in this paper regardless of the number of elastic joints or the locations of fingertip contact with the object.

Since the procedures developed are completely geometric construction based, computer graphics tools can be used in the process. This ability enables one to easily choose the configuration of each finger in a constrained space for any given hand to achieve a desired compliance.

Author contributions. Shuguang Huang and Joseph Schimmels conceived and designed the study. Huang performed the analysis and equation derivation for the problem. Huang and Schimmels wrote the article.

Financial support. This research was supported by the National Science Foundation under Grant CMMI-2024554.

Conflicts of interest. None.

Ethical considerations. None.

References

[1] D. E. Whitney, "Quasi-static assembly of compliantly supported rigid parts," *ASME J. Dyn. Syst. Meas. Control* **104**(1), 65–77 (1982).
[2] J. M. Schimmels and M. A. Peshkin, "Admittance matrix design for force guided assembly," *IEEE Trans. Robot. Autom.* **8**(2), 213–227 (1992).
[3] R. V. Ham, T. G. Sugar, B. Vanderborght, K. W. Hollander and D. Lefeber, "Compliant actuator designs: Review of actuators with passive adjustable compliance/controllable stiffness for robotic applications," *IEEE Robot. Automat. Mag*. **16**(3), 81–94 (2009).
[4] S. Huang and J. M. Schimmels, "The bounds and realization of spatial stiffnesses achieved with simple springs connected in parallel," *IEEE Trans. Robot. Autom.* **14**(3), 466–475 (1998).
[5] R. G. Roberts, "Minimal realization of a spatial stiffness matrix with simple springs connected in parallel," *IEEE Trans. Robot. Autom.* **15**(5), 953–958 (1999).
[6] K. Choi, S. Jiang and Z. Li, "Spatial stiffness realization with parallel springs using geometric parameters," *IEEE Trans. Robot. Autom.* **18**(3), 264–284 (2002).
[7] M. B. Hong and Y. J. Choi, "Screw system approach to physical realization of stiffness matrix with arbitrary rank," *ASME J. Mech. Robot*. **1**(2), 0210071–8 (2009).
[8] N. Simaan and M. Shoham, "Stiffness synthesis of a variable geometry six-degrees-of-freedom double planar parallel robot," *Int. J. Robot. Res.* **22**(9), 757–775 (2003).
[9] K. Wen, C. Shin, T. Seo and J. Lee, "Stiffness synthesis of 3-DOF planar 3RPR parallel mechanisms," *Robotica* **34**(12), 2776–2787 (2016).
[10] J. Yu, S. Li, H. Su and M. L. Culpepper, "Screw theory based methodology for the deterministic type synthesis of flexure mechanisms," *ASME J. Mech. Robot*. **3**(3), 0310081–14 (2011).
[11] Y. Du, T. Li, W. Ji, Y. Jiang and F. Li, "Compliance modeling of planar flexure-based mechanisms and its application to micro-motion stages," *Int. J. Adv. Robot. Syst.* **13**(4), 1–11 (2016).
[12] G. Krishnan, C. Kim and S. Kota, "A metric to evaluate and synthesize distributed compliant mechanisms," *ASME J. Mech. Des*. **135**(1), 0110041–9 (2013).
[13] S. Kirmse, L. F. Campanile and A. Hasse, "Synthesis of compliant mechanisms with selective compliance – An advanced procedure," *Mech. Mach. Theory* **157**(2), 104184 (2021).
[14] S. Huang and J. M. Schimmels, "Geometric construction-based realization of planar elastic behaviors with parallel and serial manipulators," *ASME J. Mech. Robot*. **9**(5), 051006(1–10) (2017).

https://doi.org/10.1017/S0263574722001448 Published online by Cambridge University Press

[15] S. Huang and J. M. Schimmels, "Geometric approach to the realization of planar elastic behaviors with mechanisms having four elastic components," *ASME J. Mech. Robot*. **10**(4), 041004(1–13) (2018).
[16] S. Huang and J. M. Schimmels, "Geometry based synthesis of planar compliances with redundant mechanisms having five compliant components," *Mech. Mach. Theory* **134**(1), 645–666 (2019).
[17] S. Huang and J. M. Schimmels, "Synthesis of planar compliances with mechanisms having six compliant components: geometric approach," *ASME J. Mech. Robot*. **12**(3), 031013(1–13) (2020).
[18] S. Huang and J. M. Schimmels, "Geometric construction-based realization of spatial elastic behaviors in parallel and serial manipulators," *IEEE Trans. Robot.* **34**(3), 764–780 (2018).
[19] K. Wang, H. Dong, C. Qiu, I. Chen and J. Dai, "Repelling-screw-based geometrical interpretation of dualities of compliant mechanisms," *Mech. Mach. Theory* **169**(104636), (2022).
[20] S. Huang and J. M. Schimmels, "Planar compliance realization with two 3-joint serial manipulators connected in parallel," *ASME J. Mech. Robot*. **14**(5), 051007(1–12) (2022).
[21] J. K. Salisbury, "Active Stiffness Control of Manipulator in Cartesian Coordinates," **In:** *IEEE 19th Conference of Decision and Control*, Albuquerque, NM, USA (December 1980) pp. 95–100.
[22] M. R. Cutkosky and I. Kao, "Computing and controlling the compliance of a robotic hand," *IEEE Trans. Robot. Autom.* **5**(2), 617–622 (1989).
[23] H. R. Choi, W. K. Chung and Y. Youm, "Stiffness analysis and control of multi-fingered robot hands," *ASME J. Dynam. Syst. Meas. Control* **117**(3), 435–439 (1995).
[24] K. B. Shimoga, "Robot grasp synthesis algorithms: A survey," *Int. J. Robot. Res.* **15**(3), 230–266 (1996).
[25] I. Kao and C. Ngo, "Properties of the grasp stiffness matrix and conservative control strategies," *Int. J. Robot. Res.* **18**(2), 159–167 (1999).
[26] K. Shimoga and A. Goldenberg, "Constructing Multifingered Grasps to Achieve Admittance Center," **In:** *IEEE International Conference on Robotics and Automation*, Nice, France (May 1992) pp. 2296–2301.
[27] B. Kim, B. Yi, S. Oh and I. Suh, "Independent finger and independent joint-based compliance control of multifingered robot hands," *IEEE Trans. Robot. Autom.* **19**(2), 185–199 (2003).
[28] J. Bimbo, E. Turco, M. G. Ardakani, M. Pozzi, G. Salvietti, V. Bo, M. Malvezzi and D. Prattichizzo, "Exploiting robot hand compliance and environmental constraints for edge grasps," *Front. Robot. AI* **6**, 1–13 (2019).
[29] S. Huang and J. M. Schimmels, "Planar compliance realized with a hand composed of multiple 2-joint fingers," *Mech. Mach. Theory* **173**(3), 104847 (2022).
[30] Y. Wei, Z. Zou, G. Wei, L. Ren and Z. Qian, "Subject-specific finite element modelling of the human hand complex: Muscle-driven simulations and experimental validation," *Ann. Biomed. Eng*. **48**(4), 1181–1195 (2020).
[31] Y. Wei, Z. Zou, Z. Qian, L. Ren and G. Wei, "Biomechanical analysis of the effect of the finger extensor mechanism on hand grasping performance," *IEEE Trans. Neur. Syst. Rehab.* **30**, 360–368 (2022).
[32] S. Huang and J. M. Schimmels, "Achieving an arbitrary spatial stiffness with springs connected in parallel," *ASME J. Mech. Des*. **120**(4), 520–526 (1998).
[33] S. Huang and J. M. Schimmels, "The duality in spatial stiffness and compliance as realized in parallel and serial elastic mechanisms," *ASME J. Dyn. Syst. Meas. Control* **124**(1), 76–84 (2002).
[34] S. Huang and J. M. Schimmels, "Realization of point planar elastic behaviors using revolute joint serial mechanisms having specified link lengths," *Mech. Mach. Theory* **103**(3), 1–20 (2016).
[35] S. C. Wiemer, Optimal Admittance Characteristics for Force-Assembly of Convex Planar Polygonal Parts, Master's thesis (Marquette University, Milwaukee, WI, USA, 2007).

Cite this article: S. Huang and J. M. Schimmels (2023). "Grasp compliance achieved with a planar hand composed of multiple 3-joint fingers", Robotica **41**, 587–608. https://doi.org/10.1017/S0263574722001448